

## Electrophilic Coordination Catalysis: A Summary of Previous Thought and a New Angle of Analysis

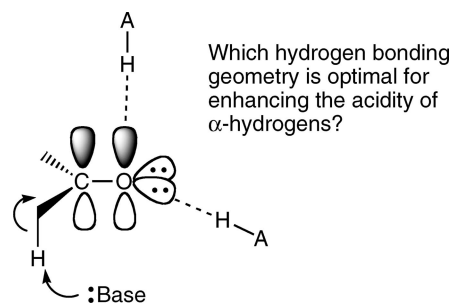
RONALD J. T. HOUK,<sup>‡</sup> ARTHUR MONZINGO,<sup>†</sup> AND  
ERIC V. ANSLYN<sup>\*,†</sup>

<sup>†</sup>Department of Chemistry and Biochemistry, The University of Texas,  
1 University Station A5300, Austin, Texas 78712, <sup>‡</sup>Sandia National Laboratories,  
7011 East Avenue, Mail Stop 9291, Livermore, California 94550-0969

RECEIVED ON MAY 23, 2007

### CON SPECTUS

One of the most common, and yet least well understood, enzymatic transformations is proton abstraction from activated carbon acids such as carbonyls. Understanding the mechanism for these proton abstractions is basic to a good understanding of enzyme function. Significant controversy has arisen over the means by which a given enzyme might facilitate these deprotonations. Creating small molecule mimics of enzymes and physical organic studies that model enzymes are good approaches to probing mechanistic enzymology. This Account details a number of molecular recognition and physical organic studies, both from our laboratory and others, dealing with the elucidation of this quandary. Our analysis launches from an examination of the active sites and proposed mechanism of several enzyme-catalyzed deprotonations of carbon acids. This analysis highlights the geometries of the hydrogen bonds found at the enzyme active sites. We find evidence to support  $\pi$ -oriented hydrogen bonding, rather than lone pair oriented hydrogen bonding. Our observations prompted us to study the stereochemistry of hydrogen bonding that activates carbonyl  $\alpha$ -carbons to deprotonation. The results from our own thermodynamic, kinetics, and computational studies, all of which are reviewed herein, suggest that an unanticipated level of intermediate stabilization occurs via an electrophilic interaction through the  $\pi$ -molecular orbital as opposed to traditional lone pair directed coordination. We do not postulate that hydrogen bonding to  $\pi$ -systems is intrinsically stronger than to lone pairs, but rather that there is a greater change in bond strength during deprotonation when the hydrogen bonds are oriented at the  $\pi$ -system. Through these studies, we conclude that many enzymes preferentially activate their carbon acid substrates through an electrophilic coordination directed towards the  $\pi$ -bond of the carbonyl rather than the conventional lone pair directed model.

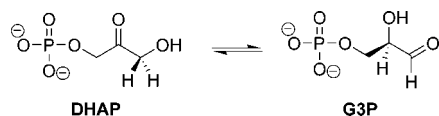


### I. Enzymatic Enolization

Enzymatic transformations that involve the removal of an  $\alpha$ -proton from a carbon acid are essential to many metabolic pathways.<sup>1</sup> To enzymologists and physical organic chemists, these reactions present a singularly interesting dilemma. How does an enzyme, working with a cadre of relatively weak acids and bases, facilitate the deprotonation of a carbon acid? The  $pK_a$ 's of typical  $\alpha$ -hydrogens range from as low as 12 to as high as 30 depending on the type of carbon acid, yet

enolases, racemases, aldolases, and various other enzyme classes readily perform  $\alpha$ -carbon proton abstractions using acids and bases with  $pK_a$ 's closer to the 6–10 range at physiological pH. To set the stage of this Account, we begin with a brief discussion of some classically studied enzymes that undergo proton transfer catalysis of carbon acids. The goal of this introduction is not to highlight the myriad controversies surrounding these enzyme mechanisms, but rather to point out some features relevant to our later discussions.

SCHEME 1



**A. Triosephosphate Isomerase.** Triosephosphate isomerase (TIM) catalyzes the interconversion of dihydroxyacetone phosphate (DHAP) to glyceraldehyde-3-phosphate (G3P) (Scheme 1).<sup>2</sup> The mechanism associated with TIM can be superficially labeled a 1,2-proton shift, and its mechanism has been thoroughly investigated.<sup>3,4</sup> The transformation is thought to proceed through a transiently stable intermediate, such as an enediolate.<sup>3</sup>

It was determined by analysis of analogue-bound crystal structures that, rather than simple general base catalysis from Glu165 (Figure 1A), the transformation proceeds via general base–general acid catalysis with potential electrophilic/acid catalytic assistance from the  $\epsilon^2$ N of a histidine residue, His95 (Figure 1A).<sup>5–7</sup> One possibility of how this assistance is

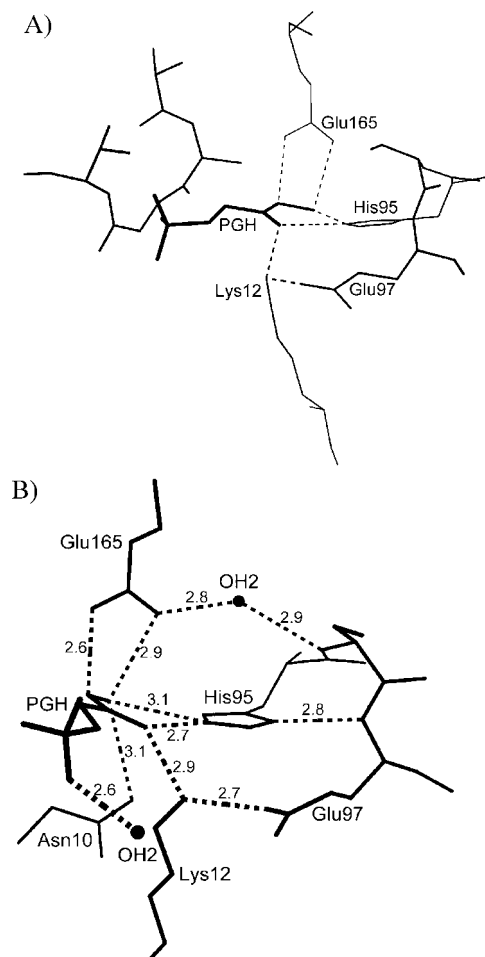
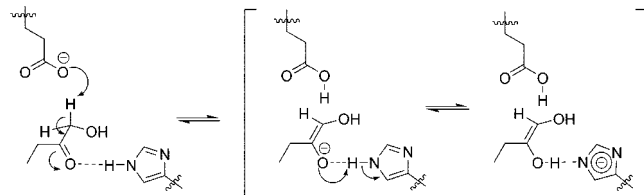
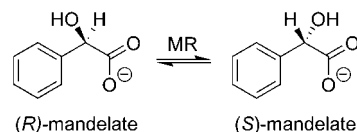


**FIGURE 1.** Active site TIM binding the analogue phosphoglycolohydroxamate (PGH). (A) Computer-generated model from the crystallographic data.<sup>5</sup> (B) Schematic of the active site residues with potential hydrogen bonds delineated.<sup>6</sup>

**SCHEME 2.** Proposed enediol route for TIM mechanism showing proton transfer from His95, although Lys12 could play a similar role



SCHEME 3



thought to occur is that the neutral imidazole from His95 gives up its proton to the intermediate to form the neutral enediol and an imidazolite anion.<sup>6</sup> The  $pK_a$  associated with this process is usually considered to be close to 14.5. However, it has been postulated that the position of His95 at the N-terminus of an  $\alpha$ -helix provides a great deal of shielding, thereby lowering this  $pK_a$  to roughly 11.5,<sup>8–10</sup> which corresponds to the estimated  $pK_a$  of the enediol intermediate. Similarly, Lys12 is proximal to the carbonyl, opposite the general base, and could supply a proton. Note in Figure 1A that Lys12 is oriented toward the  $\pi$ -system of the carbonyl. Either general acid could thus allow for rapid proton exchange from the imidazole to the intermediate (Scheme 2).<sup>10–12</sup>

**B. Mandelate Racemase.** The enzyme mandelate racemase (MR) catalyzes the  $Mg^{2+}$ -assisted interconversion of the stereoisomers of mandelate (Scheme 3). This 1,1-proton transfer has been studied in great detail and has been shown to be the result of a two-base general base mechanism.<sup>13,14</sup> Figure 2 shows a schematic of the active site of MR bound to (*S*)-mandelate extrapolated from a crystal structure of an (*R*)- $\alpha$ -phenylglycidate alkylated MR conjugate. Unlike TIM above and citrate synthase discussed below, MR requires the use of a doubly charged metal such as  $Mg^{2+}$ ,  $Co^{2+}$ ,  $Ni^{2+}$ , or  $Mn^{2+}$ .<sup>15,16</sup> The crystal structure shows interaction of the metal with the one carboxylate oxygen and the  $\alpha$ -hydroxy group.

The two general bases have been determined to be Lys166 for the *S*-enantiomer and His297 for the *R*-enantiomer.<sup>13,18</sup> The final element of the active site crucial to catalysis is the Glu317 residue.<sup>19</sup> The crystal structure analysis shows a likely hydrogen bond between the carbonyl oxygen of the mandelate carboxylate and a *neutral* glutamic acid carboxylic acid side chain.<sup>14</sup> It has been suggested that Glu317 acts as an electrophilic (general acid) catalyst in this system. The  $pK_a$  of the protonated enediolate intermediate ( $\sim 6.6$ ) and that of

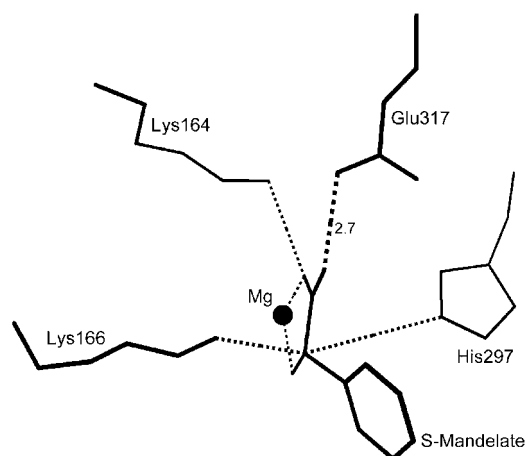


**FIGURE 2.** Active site of MR with (*S*)-mandelate shows five key elements:  $\text{Mg}^{2+}$ , Lys164, Lys166, His297, and Glu317.<sup>17</sup>

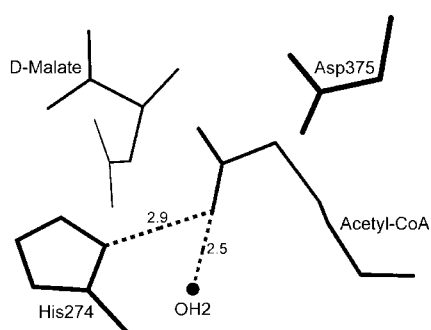


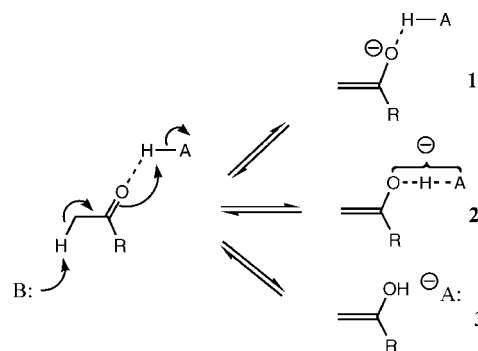
**FIGURE 3.** Active site binding of acetyl-CoA from a ternary complex of *D*-malate, acetyl-CoA, and CS. The hydrogen bond from the  $\delta^1\text{N-H}$  to the carbonyl oxygen is indicated.<sup>23</sup>

Glu317 (~6) should allow for rapid proton exchange between the acid residue and the intermediate structure to give the geminal enediol intermediate.<sup>20</sup>

**C. Citrate Synthase.** The first step of the tricarboxylic acid cycle condenses acetyl-CoA with oxaloacetate using the enzyme citrate synthase (CS).<sup>2</sup> The proposed mechanism begins with the deprotonation of the  $\alpha$ -carbon of acetyl-CoA by Asp375 with concomitant coordination/protonation of the carbonyl oxygen by His274. Claisen condensation of the resulting enol(ate) with oxaloacetate via general base–general acid (electrophilic) catalysis provided by His274 and His320 then follows.<sup>21–23</sup>

Figure 3 shows the structure of a substrate analogue *D*-malate, along with acetyl-CoA and CS, indicating the hydrogen bond from the His274  $\delta^1\text{N}$  to the carbonyl of the thioester. The carboxylate from Asp375 is poised on the opposite side of the substrate in close proximity to the methyl group and acts as a general base. The orientation of this hydrogen bond is toward the  $\pi$ -system and will become more important later in this discussion.

#### SCHEME 4



As in the case with TIM, compelling evidence that the environmental positioning of these residues causes significant altering of their  $\text{p}K_a$ 's was reported through site-directed mutagenesis studies.<sup>21,24,25</sup> Any attempt to change the active site residues resulted in dramatically increased stability against thermal denaturing. The implication is that the active site is specifically organized to electronically or sterically destabilize these residues in such a way that generates a shift in their acid/base catalyzing properties.<sup>1</sup>

## II. Electrophilic Catalysis

**A. Low Barrier Hydrogen Bonds.** A different theory for the specific role of these electrophilic general acid catalysts has been postulated by Gerlt and Gassman, as well as others.<sup>17,26–29</sup> This theory involves the formation of very short, strong hydrogen bonds between the electrophilic catalysts and the respective substrates in the transient intermediates, often called low barrier hydrogen bonds (LBHBs)<sup>30</sup> In the gas phase, crystals, and nonaqueous solvents, LBHBs have been shown to be very strong, on the order of  $\geq 20$  kcal/mol.<sup>30</sup> Several requirements are usually outlined for the possible formation of LBHBs: (1) The distance between the heteroatoms of the species must be less than 2.55 Å. A typical hydrogen bond length in water is 2.8 Å, which classifies the classic water network as a set of weak hydrogen bonds.<sup>31</sup> (2) There must be a congruity of the  $\text{p}K_a$ 's of the donor/accepter pair. (3) It has been shown that LBHBs will not form in competitive media such as water or other protic solvents. It has been strongly argued that the formation of LBHBs in enzymatic transformations is not feasible because of this last caveat.<sup>32</sup> However, calculations have shown that ordered water molecules, such as those found in enzyme active sites, will not interfere with low barrier hydrogen bonding.<sup>17</sup>

The dilemma with proton transfer catalysis, such as in the case studies discussed above, is that the calculated  $\Delta G^\ddagger$  is usually 13–17 kcal/mol in the enzyme.<sup>33,34</sup> However, on the

basis of the  $pK_a$ 's of the general bases involved in these reactions ( $\sim 6-7$ ),  $\Delta G^\ddagger$  in solution would be on the order of 20 kcal/mol greater. The question then becomes, how does the enzyme achieve this fantastic reduction in the activation energy for these carbon acid processes? Gerlt and Gassman proposed that the data for enzymes such as those discussed above provided for the formation of an intermediate that was neither the anionic enolate (**1**) nor the neutral enol (**3**), but rather a structure in between stabilized by a low barrier hydrogen bond from the electrophilic catalyst residue (**2**) (Scheme 4).<sup>17</sup>

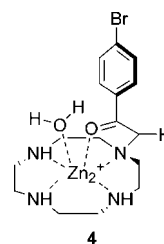
As discussed in the previous section, the near  $pK_a$  congruence of the would-be neutral enol intermediates with the perturbed general acid catalysts of the three enzymes could be interpreted to support LBHBs. Thus, by generating an intermediate with an intermolecular interaction that can reduce its free energy by up to 20 kcal/mol, the enzyme facilitates a large reduction in the  $\Delta G^\circ$  of the intermediate. The reduction of the intrinsic kinetic barrier,  $\Delta G^\ddagger_{\text{int}}$ , was proposed to arise from solvation effects of the general acid catalyst based on the principle of nonperfect synchronization (PNS).

**B. Principle of Nonperfect Synchronization.** It is well-known that the rate of deprotonation is much slower for carbon acids than acids of oxygen, sulfur, or other elements regardless of the  $pK_a$ . This observation has been attributed to PNS.<sup>35</sup> PNS effects are seen in reactions in which two or more events are occurring during the same mechanistic step, such as in the deprotonation of a carbon acid. With a heteroacid, such as  $H_3O^+$ , there is only the proton transfer occurring in the transition state. Carbon acids such as acetaldehyde or nitromethane, however, have not only a proton transfer but also a delocalization of charge through resonance and a rehybridization of the resulting carbanion. The result is a situation in which one or more processes lag behind another on the reaction coordinate.

Perhaps the most widely known study of PNS has been termed the nitroalkane anomaly.<sup>36,37</sup> Brønsted analysis of the deprotonation of various aryl nitroalkanes with hydroxide revealed highly irregular  $\alpha$ - and  $\beta$ -values of 1.54 and  $-0.55$ , respectively. Since the Brønsted coefficients can be thought of as a measure of the extent of proton transfer at the transition state, a 1.54  $\alpha$ -value suggests nearly complete deprotonation at the TS in the forward direction, and the  $-0.55$   $\beta$ -value implies nearly no protonation in the reverse direction. The conclusion is that proton transfer happens first while rehybridization and delocalization through resonance lags behind. This asynchronicity results in a localization of charge on the carbon, which raises the intrinsic kinetic barrier as a result of the high unfavorability of anionic carbon.

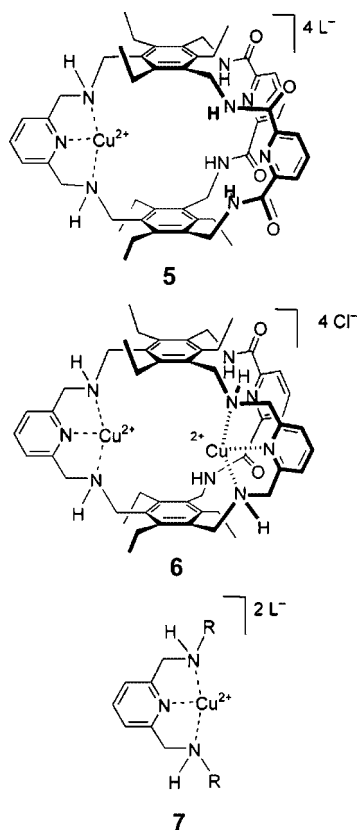
There have also been studies on the effects of solvation on the extent of asynchronous proton transfer. In hydrogen bonding solvents the PNS effect is larger than in nonanion stabilizing solvents such as DMSO and acetonitrile.<sup>35</sup> The reason for this solvent dependence is that solvent reorganization in hydrogen bonding solvents also lags behind charge transfer. Hence, in a solvent that reorients itself around a charge, there is an added contribution to the  $\Delta G^\ddagger_{\text{int}}$  from the entropic cost of solvent reorientation. Gerlt and Gassman argued that the electrophilic general acid residues in enzymes are preoriented to "solvate" the growing negative charge on the oxygen at the transition state whether it formed a LBHB or not.<sup>17</sup> The preorientation would eliminate the entropic cost of solvent reorientation and remove it from  $\Delta G^\ddagger_{\text{int}}$ .

**C. Metal Coordination.** The low barrier hydrogen bond theory has had several critics, and articles continue to be published that claim to show evidence either for or against the formation of LBHBs in enzyme mechanisms.<sup>38-45</sup> Several other theories have been proposed, either in lieu of or complementary to the formation of LBHBs. One of these is the theory that metal coordination in enzymes plays a much larger role in reducing the overall kinetic barrier by reducing the  $pK_a$  of the  $\alpha$ -proton. Enolases, racemases, and aldolases in particular all contain at least one vital metal center at their active sites. Kimura et al. synthesized the 4-bromophenacyl-pendant cyclen system **4** to evaluate the mechanism of class II aldolases and the role of Zn(II) in the enolization step.<sup>46</sup> The presence of the Zn(II) in close proximity of the carbonyl oxygen in **4** was able to reduce the  $pK_a$  of the  $\alpha$ -proton to 8.41, nearly 10 orders of magnitude. The kinetic barrier toward deprotonation also appeared to be reduced with the half-life of H-D exchange reported to be 25 min at 298 K.



Studies in our group using a series of hosts **5-7** have shown that shifts of nearly 12  $pK_a$  units are observed for  $\alpha$ -hydrogens of various  $\beta$ -diketones.<sup>47</sup> The bicyclic hosts **5** and **6** showed slightly greater  $pK_a$  reduction due to better solvent exclusion from the interior, yet in all cases, coordination to the Cu(II) affords a great deal of enolate stabilization. However, these findings do not account for enzymes such as TIM and

CS in which no metals are present at the active site of enol-(ate) formation.



### III. The Third Dimension

Over the past decade, our group has studied an interesting stereochemical phenomenon of electrophilic catalysis. The crystal structure of wild-type medium chain acyl-CoA dehydrogenase (Figure 4A) shows no metal coordination in the active site, yet the substrate, like those in TIM, MR, and CS, must be highly activated for  $\alpha$ -deprotonation to occur.<sup>48</sup> The hydrogen bonds indicated to the carbonyl oxygen are somewhat distorted from conventional lone pair directed models. Instead, the interactions from the backbone amide of Glu376 and the 2'-OH of the flavin are oriented toward the  $\pi$ -system. Likewise, 4-chlorobenzoyl-CoA dehalogenase (Figure 4B) catalyzes the hydrolytic removal of chloride from 4-chlorobenzoyl-CoA conjugates through a Meisenheimer complex (Figure 4C).<sup>49</sup> Again, the backbone amide hydrogen bonds are not in the plane described by the carbonyl oxygen's lone pairs but are directed toward the C-O  $\pi$ -bond. In addition, in the case of *o*-succinylbenzoate synthetase, Gerlt proposed that a Lys opposite the face of the substrate from the general base assists activation, although they did not draw specific attention to this unusual orientation.<sup>50</sup>

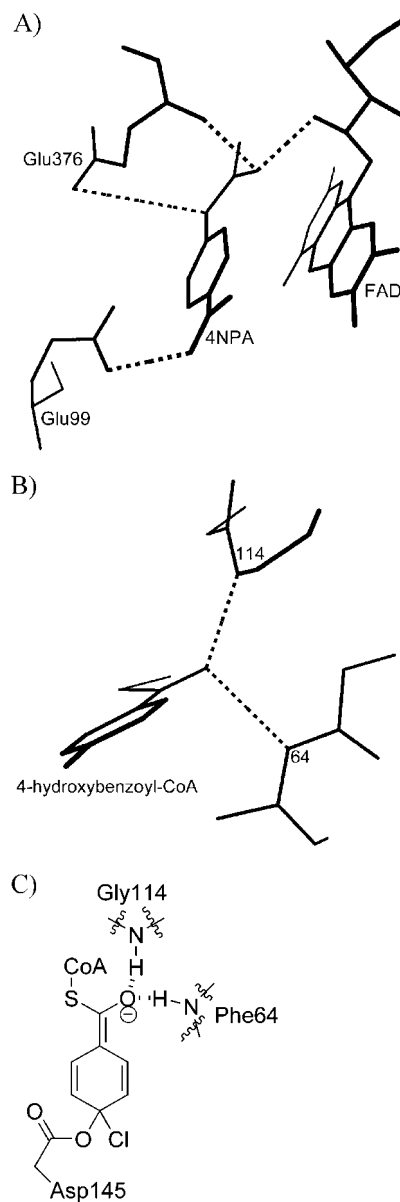
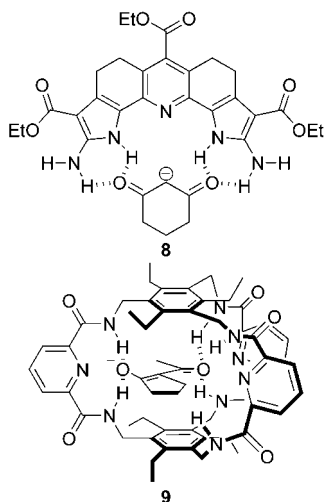


**FIGURE 4.** (A) 4-(Nitrophenyl)acetyl-CoA bound to MCADH with  $\pi$ -directed hydrogen bonds to the substrate analogue.<sup>48</sup> (B) Active site of 4-chlorobenzoyl-CoA dehalogenase with backbone amide hydrogen bonds to the  $\pi$ -face of the thioester.<sup>49</sup> (C) Enolic structure of the Meisenheimer intermediate from the mechanism of 4-chlorobenzoyl-CoA dehalogenase.

Similarly, if we look back at the three case studies discussed earlier, there are analogous stereochemical orientations. Citrate synthase exhibits the most obvious  $\pi$ -coordinative character. The crystal structure, Figure 3, shows a good deal of hydrogen bonding from His274 to the  $\pi$ -bond of the carbonyl. A similar case can be made for TIM. The crystal structures in Figure 1 show possible electrophilic interaction toward the  $\pi$ -system of the substrates from the side-chain Asp10 amide and the  $\epsilon$ -amine of Lys12. The crystal structure of mandelate racemase, Figure 2, is somewhat anomalous to this discussion.

However, of all the enzymes discussed here, MR is the only instance in which an active site metal is vital to affect catalysis. For the remainder of this Account, we will focus on our efforts toward the elucidation of the effect of the stereochemical orientation of electrophilic coordination on the kinetics and thermodynamics of carbon acid deprotonation.

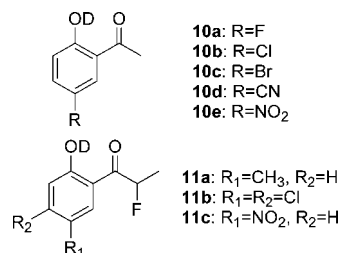
**A. Thermodynamic Effects.** We have studied the ability of hydrogen bonding to affect the thermodynamics of carbon acid deprotonation as a function of geometry by using several model systems.<sup>51,52</sup> For example, the crescent shaped receptor **8** utilizes four amide-like hydrogen bond donors in a cavity to emulate an enzyme active site. Receptor **8** was most complementary to 1,3-cyclohexanedione, with an association constant ( $K_a$ ) of  $1.35 \times 10^4 \text{ M}^{-1}$  in acetonitrile. However, even with the cooperative binding of four hydrogen bonds, potentiometric titrations revealed that **8** was only able to lower the  $pK_a$  of 1,3-cyclohexanedione by about 1 unit.<sup>53</sup>



The bicyclic cyclophane **9** was used in a later study to test the effect of  $\pi$ -orbital hydrogen bond acceptance on  $pK_a$  shifting.<sup>51</sup> In this study, 2-acetylcyclopentanone had the greatest complementarity to **9** ( $K_a = 3.06 \times 10^3 \text{ M}^{-1}$ ), and was chosen as the model carbon acid. The binding cavity of **9** is small enough (7.0 Å high) to constrain the guest to a horizontal orientation, which also constrains the hydrogen bonds to  $\pi$ -donation. In acetonitrile, the  $pK_a$  of 2-acetylcyclopentanone in the presence of **9** was reduced by nearly 3 units, constituting a 300% increase in the stabilization of enolate formation based largely on the geometry of hydrogen bonding.

**B. Kinetic Stabilization.** The previous two studies, although informative, are based solely on the thermodynamic advantages of hydrogen bond orientation. To determine the effects of lone pair directed hydrogen bonding on the kinetics of  $\alpha$ -proton abstraction, we developed a series of

2-acetylphenol probes **10** and **11** for analysis of the rate of H–D exchange at the active carbon.<sup>54</sup> As a control, the phenol methyl ether versions of each compound in the **10** series were also synthesized and subjected to rate studies.



The kinetics experiments were conducted via <sup>1</sup>H NMR in both 4:1 CD<sub>3</sub>OD/D<sub>2</sub>O (pD 5.83) and in acetonitrile. The  $pK_a$ 's of the phenols were determined in both the methanol/water mixture (potentiometrically) and in acetonitrile (by comparison with known indicators). The Brønsted plots of series **10** and the methyl-ether analogues showed the relative rate enhancement over the entire series to be less than a single log unit, which is quite low for an intramolecular hydrogen bond.<sup>55</sup> Also, the  $\alpha$ -values in water determined from the slopes of the **10** series and the methyl ether controls are only 0.24 and 0.15, respectively. The difference of these two values gives a measure of the effect of hydrogen bond strength on the rate constant and only amounts to 0.09 in both protic and aprotic media. The **11** series was used to determine if lowering the  $pK_a$  of the enol intermediate would result in a greater effect due to better  $pK_a$  matching for possible LBHB formation. The results showed similar independence on the strength of the hydrogen bond, giving an  $\alpha$ -value of 0.24 in acetonitrile based on  $pK_a$ 's determined in water.

These results were attributed to PNS effects. Because there is very little negative charge developing on the carbonyl oxygen at the transition state of deprotonation, the overall strength of a hydrogen bond directed through a nonparticipating orbital would make little difference to the activation barrier. The chief extrapolation to enzyme behavior is that the formation of a strong coordination to the lone pair electrons of the substrate carbonyl would have very little effect on  $\Delta G^\ddagger$ .

**C. Lithium-Acetaldehyde Model.** One ultimate goal of our research is to examine whether placing a strong electrophilic coordination directed toward the  $\pi$ -electron density could have a greater effect not only on the thermodynamic stability of the resulting enol(ate) but also on the kinetics by augmenting the extent of charge delocalization at the transition state. To semiquantitatively assess the extent of this effect, we recently performed a series of computational

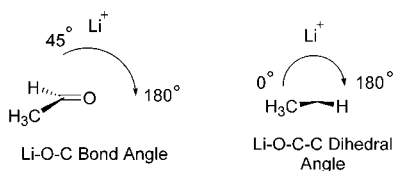


**FIGURE 5.** Surfaces were obtained by iteration in  $5^\circ$  increments along both the Li–O–C bond angle (left) from  $45^\circ$  to  $180^\circ$  and the Li–O–C–C dihedral angle (right) from  $0^\circ$  to  $180^\circ$ .

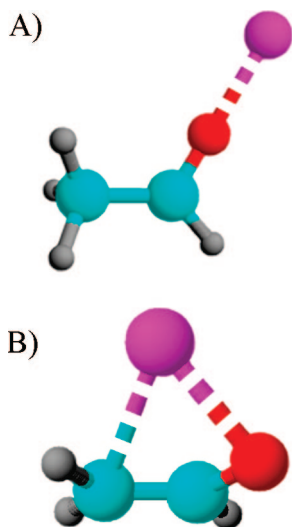


**FIGURE 6.** Structural representations of the global energy minimum geometries obtained from potential energy surfaces of the  $\text{Li}^\oplus$ –acetaldehyde (A) and  $\text{Li}^\oplus$ –enolate (B) systems.<sup>56</sup>

studies on a simple electrophile coordinating to a simple carbon acid.<sup>56</sup> A series of previous studies have examined electrophilic coordination to enolate anions and their associated conjugate acids, but these studies did not focus on predicting the best orientation to enhance acidities of the  $\alpha$ -hydrogens.<sup>57</sup>

We chose the simplest nonproton electrophile,  $\text{Li}^\oplus$ , and the simplest carbon acid, acetaldehyde. Two potential energy surfaces were generated at an MP2 level with a 6-31G\* basis set using the ACES II quantum chemical program package developed by Stanton and collaborators.<sup>58</sup> The surfaces were generated by manually varying the Li–O–C bond angle against the Li–O–C–C dihedral angle in  $5^\circ$  increments as shown in Figure 5.

Two surfaces were generated as composites of single-point energies for each combination of bond and dihedral angles listed in Figure 5, one for neutral acetaldehyde and the other for its enolate. The global energy minimum geometries predicted from these analyses are shown in Figure 6. As was expected for neutral acetaldehyde, the global energy minimum geometry (Figure 6A) shows coordination of the lithium solely to the longitudinal lone pair of the carbonyl oxygen.

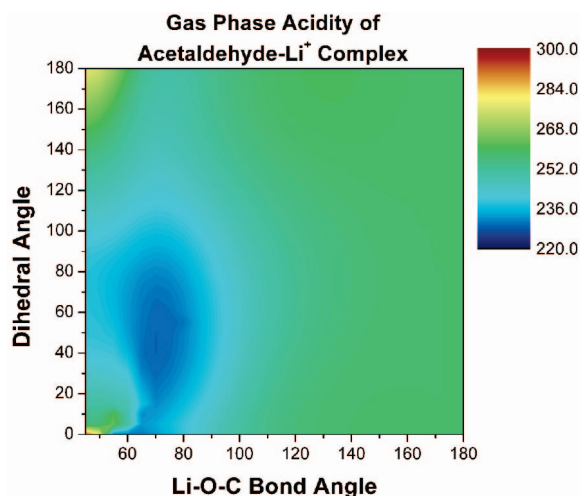


**FIGURE 7.** Gas-phase acidity (kcal/mol) analysis of the acetaldehyde– $\text{Li}^\oplus$  complex derived as the difference of the acetaldehyde and enolate surfaces.<sup>56</sup>

Interestingly, the global energy minimum geometry found from the enolate surface is quite different. In this case, the minimum geometry occurs at a Li–O–C bond angle of  $85^\circ$  and a Li–O–C–C dihedral angle of  $45^\circ$  (Figure 6B). The first aspect to notice is the out-of-plane dihedral angle. This geometry suggests a significant amount of  $\pi$ -system coordination in the enolate system. The second important facet of this model is that, based on rudimentary resonance analysis, this energy minimum arises as a result of coordination of the lithium ion to the two centers of negative charge—the oxygen and  $\alpha$ -carbon. The optimum geometry derived from the surface calculations (Figures 5 and 6) are similar to ones found via single point calculations.<sup>59</sup>

These two analyses alone say very little about which geometry is best to generate a substantive shift in the acid dissociation constant,  $K_a$ . The contour plot shown in Figure 7 is the difference of the enthalpies of lithium coordination to acetaldehyde and its corresponding enolate and gives a measure of the gas-phase acidity of this system. Figure 7 does not technically represent a potential energy surface but rather should be thought of as a measure of the acid dissociation potential at each given geometry. This acidity analysis reveals a new minimum occurring at  $70^\circ$ , while the dihedral angle remains  $45^\circ$  (Figure 8). The lithium now resides antiperiplanar to the cleaving  $\alpha$ -hydrogen. This geometry represents a double threat: backside electrophilic coordination to the orbital of the breaking C–H bond and  $\pi$ -system coordination to the carbonyl. Both of these effects would lead to an arguably more labile proton.

This calculated configuration (Figure 8) is in sharp contrast with the normally accepted geometry for enhancing acidity. The difference in acidity between this new geometry and the

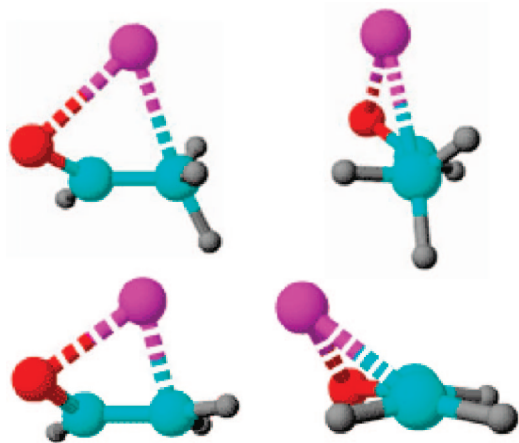


**FIGURE 8.** (top) Front and side views of the optimum geometry for lithium coordination to enhance the acidity of acetaldehyde. (bottom) Analogous views of the enolate complex.<sup>54</sup>

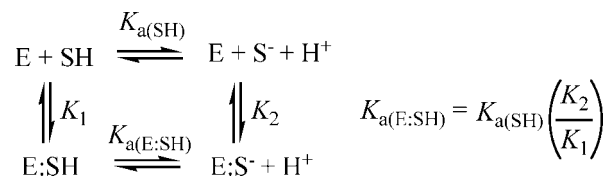
traditional model amounts to roughly 28.9 kcal/mol. At 0 K, this value results in a roughly 20 unit greater shift in  $pK_a$  with  $\pi$ -directed coordination.

In addition, the discovery of the maximum acidity enhancement occurring at a coordination geometry in which the electrophile is heavily coordinated to the  $\alpha$ -carbon is of note in light of the PNS. The effect of this coordination appears to be 2-fold. First, a destabilizing interaction through backside C–H coordination increases the lability of the proton. Notice that the C–H bond in question is elongated, indicating a weaker bond. Second, because the main contribution to the kinetic barrier of carbon acid deprotonation is the buildup of negative charge on the  $\alpha$ -carbon, coordination of an electrophile directly toward that building charge would help to significantly reduce  $\Delta G_{int}^\ddagger$ , which was suggested to be necessary by Gerlt and Gassman.<sup>17</sup>

Of course, the nearly 29 kcal/mol difference in acidity depending on the orientation of lithium coordination will be diminished in a raised dielectric medium such as that present in an enzyme active site. We have previously noted via analogy to studies of  $\alpha$ -hydrogen acidity activation in water by other Lewis acids that one would expect at least a 30–40% attenuation of the effect upon solvation by water.<sup>60</sup>

**D. Cyclic Equilibria.** As a final vantage point on our postulate of increasing  $\alpha$ -hydrogen acidity via electrophilic coordination to the  $\pi$ -system of the carbonyl, consider Scheme 5. This cyclic equilibrium shows coordination of a catalyst (E) to an acid SH followed by deprotonation. The acidity of the catalyst–acid complex ( $K_{a(E:SH)}$ ) is found to be directly proportional to the acidity of the acid ( $K_{a(SH)}$ ) and the ratio of the binding constants for the conjugate base ( $K_2$ ) to the acid ( $K_1$ ). Therefore, weakening the binding of SH with increased binding of  $S^-$  leads to increased acidity of SH. It is the ratio of

**SCHEME 5.** Cyclic equilibria showing the relationship between acidities and binding of carbonyl groups to electrophilic catalysts (E)



binding constants that is important. Therefore, our postulate does not mean that hydrogen bonding or other kinds of electrophilic coordination are intrinsically stronger when oriented at the  $\pi$ -system. Instead, our theory simply means that there is enhanced binding of the conjugate base relative to the acid when the electrophile is orientated at the  $\pi$ -system relative to being orientated at the lone pair electrons.<sup>61</sup>

## IV. Summary and Outlook

Traditionally, interactions such as ion pairing, standard hydrogen bonding (not LBHBs), and dipole–dipole interactions have been lumped together as Coulombic forces. However, this designation has led many to ignore the fact that whereas Coulomb's law is a one-dimensional function, nearly all of the so-called Coulombic forces are inherently two- or three-dimensional. Conventional descriptions of catalysis induced by electrophilic coordination, not only carbon acid deprotonation but any Lewis acid assisted transformation, tend to minimize the effects of these extra dimensions. Through the research conducted in our laboratories over the past decade, we have shown that by taking those dimensions into account, a different understanding of these processes can be achieved. Speaking specifically of carbon acid deprotonation, our studies suggest that for efficient electrophile-assisted catalysis or stabilization to be achieved, the traditionally assumed directionality of coordination to carbonyls is not optimal. For example, lone pair directed hydrogen bonds were shown to be rather ineffectual in the kinetic enhancement of this process, whereas the thermodynamic favorability of  $\pi$ -system/ $\alpha$ -carbon directed coordination is clearly evident from our molecular recognition studies and our computational analysis.

From this evidence, we propose a complimentary theory that, in the highly ordered environment of an enzyme active site, the formation of structures that show  $\pi$ -oriented electrophilic interactions enhance kinetic and thermodynamic stabilization more than structures with lone pair oriented interactions. Several of the enzymes we have discussed specifically in this Account show a preorganized aptitude for formation of  $\pi$ -directed coordination complexes. It is important to note that not all members of the acyl dehydrogenase (such as



citrate synthetase)<sup>62</sup> and enoyl-CoA (such as 4-chlorobenzoyl-CoA dehydrogenase)<sup>63</sup> super families, as well as others, have obvious electrophilicities in the position we are postulating is beneficial. Presumably other mechanisms of activation are at play, but this does not refute the potential benefit we put forth. Future studies on this phenomenon must include an understanding of the kinetic effects of the orientation of electrophilic coordination, and efforts are currently being pursued in our laboratories to that end.

*We would like to acknowledge the efforts of previous co-workers and collaborators: John Stanton, Vincent Lynch, Anne Kelly Rowley, Timothy Snowden, Adrian Bisson, Michael Best, Zhenlin Zhong, Robert Hanes, Brenda Postnikova, and Yannick Bomble. This research has been supported by the National Institutes of Health (GM 65515), The Welch Foundation, and the University of Texas.*

#### BIOGRAPHICAL INFORMATION

**Eric V. Anslyn** is the Norman Hackerman Professor and a University Distinguished Teaching Professor.

**Arthur Monzingo** is a research associate in the group of Dr. Jon Robertus.

**Ronald J. T. Houk** received his B.S. degree from the College of William and Mary and his Ph.D. from UT Austin. He currently holds a postdoctoral fellowship at Sandia National Laboratories.

#### FOOTNOTES

\*E-mail: anslyn@ccwf.cc.utexas.edu.

#### REFERENCES

- Remington, S. J. Mechanisms of citrate synthase and related enzymes (triose phosphate isomerase and mandelate racemase). *Curr. Opin. Struct. Biol.* **1992**, *2*, 730–735.
- Voet, D.; Voet, J. G. *Biochemistry*, 3rd ed.; John Wiley & Sons Inc.: Hoboken, NJ, 2004.
- Albery, W. J.; Knowles, J. R. Free-energy profile for the reaction catalyzed by triosephosphate isomerase. *Biochemistry* **1976**, *15*, 5627–5631.
- Rieder, S. V.; Rose, I. A. Mechanism of the triose phosphate isomerase reaction. *J. Biol. Chem.* **1959**, *234*, 1007–1010.
- Komives, E. A.; Chang, L. C.; Lolis, E.; Tilton, R. F.; Petsko, G. A.; Knowles, J. R. Electrophilic catalysis in triosephosphate isomerase: the role of histidine-95. *Biochemistry* **1991**, *30*, 3011–3019.
- Davenport, R. C.; Bash, P. A.; Seaton, B. A.; Karplus, M.; Petsko, G. A.; Ringe, D. Structure of the triosephosphate isomerase-phosphoglycolohydroxamate complex: an analog of the intermediate on the reaction pathway. *Biochemistry* **1991**, *30*, 5821–5826.
- Belasco, J. G.; Knowles, J. R. Direct observation of substrate distortion by triosephosphate isomerase using Fourier transform infrared spectroscopy. *Biochemistry* **1980**, *19*, 472–477.
- Creighton, T. E. *Proteins: Structures and Molecular Properties*, 2nd ed.; W. H. Freeman and Company: New York, 1993.
- Hol, W. G. J. The role of the  $\alpha$ -helix dipole in protein function and structure. *Prog. Biophys. Mol. Biol.* **1985**, *45*, 149–195.
- Lodi, P. J.; Knowles, J. R. Neutral imidazole is the electrophile in the reaction catalyzed by triosephosphate isomerase: structural origins and catalytic implications. *Biochemistry* **1991**, *30*, 6948–6956.
- Bruice, T. C.; Schmir, G. L. Imidazole catalysis. II. The reaction of substituted imidazoles with phenyl acetates in aqueous solution. *J. Am. Chem. Soc.* **1958**, *80*, 148–156.
- Chiang, Y.; Kresge, A. J. Enols and other reactive species. *Science* **1991**, *253*, 395–400.
- Powers, V. M.; Koo, C. W.; Kenyon, G. L.; Gerlt, J. A.; Kozarich, J. W. Mechanism of the reaction catalyzed by mandelate racemase. 1. Chemical and kinetic evidence for a two-base mechanism. *Biochemistry* **1991**, *30*, 9255–9263.
- Landro, J. A.; Gerlt, J. A.; Kozarich, J. W.; Koo, C. W.; Shah, V. J.; Kenyon, G. L.; Neidhart, D. J.; Fujita, S.; Petsko, G. A. The role of lysine 166 in the mechanism of mandelate racemase from *Pseudomonas putida*: Mechanistic and crystallographic evidence for stereospecific alkylation by (*R*)- $\alpha$ -phenylglycidate. *Biochemistry* **1994**, *33*, 635–643.
- Fee, J. A.; Hegeman, G. D.; Kenyon, G. L. Mandelate racemase from *Pseudomonas putida*. Subunit composition and absolute divalent metal ion requirement. *Biochemistry* **1974**, *13*, 2528–2532.
- Kenyon, G. L.; Hegeman, G. D. Mandelate racemase. *Adv. Enzymol. Relat. Areas Mol. Biol.* **1979**, *50*, 325–360.
- Gerlt, J. A.; Gassman, P. G. Understanding the rates of certain enzyme-catalyzed reactions: Proton abstraction from carbon acids, acyl transfer reactions, and displacement reactions of phosphodiester. *Biochemistry* **1993**, *32*, 11943–11952.
- Kallarakal, A. T.; Mitra, B.; Kozarich, J. W.; Gerlt, J. A.; Clifton, J. R.; Petsko, G. A.; Kenyon, G. L. Mechanism of the reaction catalyzed by mandelate racemase: Structure and mechanistic properties of the K166R mutant. *Biochemistry* **1995**, *34*, 2788–2797.
- Mitra, B.; Kallarakal, A. T.; Kozarich, J. W.; Gerlt, J. A.; Clifton, J. R.; Petsko, G. A.; Kenyon, G. L. Mechanism of the reaction catalyzed by mandelate racemase: Importance of electrophilic catalysis by glutamic acid 317. *Biochemistry* **1995**, *34*, 2777–2787.
- Chiang, Y.; Kresge, A. J.; Pruszyński, P.; Schepp, N. P.; Wirz, J. Mandelic acid enols: determination of the acidity in aqueous solutions and estimation of keto-enol equilibrium constants and CH acidity of mandelic acid. *Angew. Chem.* **1990**, *102*, 810–812.
- Alter, G. M.; Casazza, J. P.; Zhi, W.; Nemeth, P.; Srere, P. A.; Evans, C. T. Mutation of essential catalytic residues in pig citrate synthase. *Biochemistry* **1990**, *29*, 7557–7563.
- Karpusas, M.; Branchaud, B.; Remington, S. J. Proposed mechanism for the condensation reaction of citrate synthase: 1.9-Å structure of the ternary complex with oxaloacetate and carboxymethyl coenzyme A. *Biochemistry* **1990**, *29*, 2213–2219.
- Karpusas, M.; Holland, D.; Remington, S. J. 1.9-Å Structures of ternary complexes of citrate synthase with D- and L-malate: Mechanistic implications. *Biochemistry* **1991**, *30*, 6024–6031.
- Man, W. J.; Li, Y.; O'Connor, C. D.; Wilton, D. C. Conversion of citrate synthase into citryl-CoA lyase as a result of mutation of the active-site aspartic acid residue to glutamic acid. *Biochem. J.* **1991**, *280*, 521–526.
- Zhi, W.; Srere, P. A.; Evans, C. T. Conformational stability of pig citrate synthase and some active-site mutants. *Biochemistry* **1991**, *30*, 9281–9286.
- Cleland, W. W.; Kreevoy, M. M. Low-barrier hydrogen bonds and enzymic catalysis. *Science* **1994**, *264*, 1887–1890.
- Frey, P. A. Low-barrier hydrogen bonds. *Science* **1995**, *268*, 189.
- Frey, P. A.; Whitt, S. A.; Tobin, J. B. A low-barrier hydrogen bond in the catalytic triad of serine proteases. *Science* **1994**, *264*, 1927–1930.
- Gerlt, J. A.; Gassman, P. G. An explanation for rapid enzyme-catalyzed proton abstraction from carbon acids: importance of late transition states in concerted mechanisms. *J. Am. Chem. Soc.* **1993**, *115*, 5928–5934.
- Hibbert, F.; Emsley, J. Hydrogen bonding and chemical reactivity. *Adv. Phys. Org. Chem.* **1990**, *26*, 255–279.
- Cleland, W. W. Low-barrier hydrogen bonds and enzymic catalysis. *Arch. Biochem. Biophys.* **2000**, *382*, 1–5.
- Warshel, A.; Papazyan, A. Energy considerations show that low-barrier hydrogen bonds do not offer a catalytic advantage over ordinary hydrogen bonds. *Proc. Natl. Acad. Sci. U.S.A.* **1996**, *93*, 13665–13670.
- Marcus, R. A. Unusual slopes of free energy plots in kinetics. *J. Am. Chem. Soc.* **1969**, *91*, 7224–7225.
- Cohen, A. O.; Marcus, R. A. Slope of free energy plots in chemical kinetics. *J. Phys. Chem.* **1968**, *72*, 4249–4256.
- Bernasconi, C. F. The principles of nonperfect synchronization. *Adv. Phys. Org. Chem.* **1992**, *27*, 119–238.
- Bordwell, F. G.; Boyle, W. J., Jr. Kinetic isotope effects for nitroalkanes and their relation to transition-state structure in proton-transfer reactions. *J. Am. Chem. Soc.* **1975**, *97*, 3447–3452.
- Bordwell, F. G.; Boyle, W. J., Jr. Acidities, Bronsted coefficients, and transition state structures for 1-arylnitroalkanes. *J. Am. Chem. Soc.* **1972**, *94*, 3907–3911.

- 38 Frey, P. A. Isotope effects in the characterization of low barrier hydrogen bonds. In *Isotope Effects in Chemistry and Biology*; Taylor & Francis: Boca Raton, 2006; pp 975–993.
- 39 Fuhrmann, C. N.; Daugherty, M. D.; Agard, D. A. Subangstrom crystallography reveals that short ionic hydrogen bonds, and not a His-Asp low-barrier hydrogen bond, stabilize the transition state in serine protease catalysis. *J. Am. Chem. Soc.* **2006**, *128*, 9086–9102.
- 40 Ishida, T. Low-barrier hydrogen bond hypothesis in the catalytic triad residue of serine proteases: Correlation between structural rearrangement and chemical shifts in the acylation process. *Biochemistry* **2006**, *45*, 5413–5420.
- 41 Pasqualato, S.; Cherfils, J. Crystallographic evidence for substrate-assisted GTP hydrolysis by a small GTP binding protein. *Structure* **2005**, *13*, 533–540.
- 42 Warshel, A. Calculations of enzymatic reactions: calculations of  $pK_a$ , proton transfer reactions, and general acid catalysis reactions in enzymes. *Biochemistry* **1981**, *20*, 3167–3177.
- 43 Warshel, A.; Aqvist, J. Electrostatic energy and macromolecular function. *Annu. Rev. Biophys. Biophys. Chem.* **1991**, *20*, 267–298.
- 44 Warshel, A.; Levitt, M. Theoretical studies of enzymic reactions: dielectric, electrostatic and steric stabilization of the carbonium ion in the reaction of lysozyme. *J. Mol. Biol.* **1976**, *103*, 227–249.
- 45 Yang, W.; Drueckhammer, D. G. Computational study of the citrate synthase catalyzed deprotonation of acetyl-Coenzyme A and fluoroacetyl-Coenzyme A: Demonstration of a layered quantum mechanical approach. *J. Phys. Chem. B* **2003**, *107*, 5986–5994.
- 46 Kimura, E.; Kitamura, H.; Koike, T.; Shiro, M. Facile and selective electrostatic stabilization of uracil N(1)- anion by a proximate protonated amine: A chemical implication for why uracil N(1) is chosen for glycosylation site. *J. Am. Chem. Soc.* **1997**, *119*, 10909–10919.
- 47 Zhong, Z.; Postnikova, B. J.; Hanes, R. E.; Lynch, V. M.; Anslyn, E. V. Large  $pK_a$  shifts of  $\alpha$ -carbon acids induced by copper(II) complexes. *Chem.—Eur. J.* **2005**, *11*, 2385–2394.
- 48 Vock, P.; Engst, S.; Eder, M.; Ghisla, S. Substrate activation by acyl-Coenzyme A dehydrogenases: Transition-state stabilization and  $pK_s$  of involved functional groups. *Biochemistry* **1998**, *37*, 1848–1860.
- 49 Benning, M. M.; Taylor, K. L.; Liu, R. Q.; Yang, G.; Xiang, H.; Wesenberg, G.; Dunaway-Mariano, D.; Holden, H. M. Structure of 4-chlorobenzoyl coenzyme A dehalogenase determined to 1.8 Å resolution: An enzyme catalyst generated via adaptive mutation. *Biochemistry* **1996**, *35*, 8103–8109.
- 50 (a) Thompson, T. B.; Garrett, J. B.; Taylor, E. A.; Meganathan, R.; Gerlt, J. A.; Rayment, I. Evolution of enzymatic activity in the enolase superfamily: Structure of *o*-succinylbenzoate synthase from *Escherichia coli* in complex with  $Mg^{2+}$  and *o*-succinylbenzoate. *Biochemistry* **2000**, *39*, 10662–10676. (b) Klenchin, V. A.; Ringia, T.; Gerlt, H. A.; Rayment, I. Evolution of enzymatic activity in the enolase superfamily: Structural and mutagenic studies of the mechanism of the reaction catalyzed by *o*-succinylbenzoate synthase from *Escherichia coli*. *Biochemistry* **2003**, *42*, 14427–14433.
- 51 Snowden, T. S.; Bisson, A. P.; Anslyn, E. V. A Comparison of  $NH-\pi$  versus lone pair hydrogen bonding effects on carbon acid  $pK_a$  shifts. *J. Am. Chem. Soc.* **1999**, *121*, 6324–6325.
- 52 Snowden, T. S.; Bisson, A. P.; Anslyn, E. V. Artificial receptors involved in enolization and  $pK_a$  shifts. *Bioorg. Med. Chem.* **2001**, *9*, 2467–2478.
- 53 Kelly-Rowley, A. M.; Lynch, V. M.; Anslyn, E. V. Molecular recognition of enolates of active methylene compounds in acetonitrile. The interplay between complementarity and basicity and the use of hydrogen bonding to lower guest  $pK_a$ 's. *J. Am. Chem. Soc.* **1995**, *117*, 3438–3447.
- 54 Zhong, Z.; Snowden, T. S.; Best, M. D.; Anslyn, E. V. Rate of enolate formation is not very sensitive to the hydrogen bonding ability of donors to carboxyl oxygen lone pair acceptors; A ramification of the principle of non-perfect synchronization for general-base-catalyzed enolate formation. *J. Am. Chem. Soc.* **2004**, *126*, 3488–3495.
- 55 Hartwell, E.; Hodgson, D. R. W.; Kirby, A. J. Exploring the limits of efficiency of proton-transfer catalysis in models and enzymes. *J. Am. Chem. Soc.* **2000**, *122*, 9326–9327.
- 56 Houk, R. J. T.; Anslyn, E. V.; Stanton, J. F. Carbonyl coordination chemistry from a new angle: A computational study of  $\alpha$ -carbon acidity based on electrophile coordination geometry. *Org. Lett.* **2006**, *8*, 3461–3463.
- 57 (a) Dixon, D. A.; Eades, R. A.; Frey, R.; Gassman, P. G.; Hendewerk, M. L.; Paddon-Row, M. N.; Houk, K. N. Theoretical evaluation of the effect of electron-withdrawing substituents on carbocation stabilities. Delocalization of charge to the carbonyl and cyano groups. *J. Am. Chem. Soc.* **1984**, *106*, 3885–3891. (b) Kaufmann, E.; Schleyer, P. V. R. Ab initio mechanisms for the addition of  $CH_3Li$ ,  $HLi$ , and their dimers to formaldehyde. *J. Am. Chem. Soc.* **1985**, *107*, 5560–5562. (c) Bernasconi, C. F.; Wenzel, P. J. Is there a transition-state imbalance for proton transfers in the gas phase? An ab initio study of the carbon-to-carbon proton transfer from acetaldehyde to its enolate ion. *J. Am. Chem. Soc.* **1994**, *116*, 5405–5413. (d) Saunders, W. Ab initio and semi-empirical investigation of gas-phase carbon acidity. *J. Phys. Org. Chem.* **1994**, *7*, 268–271. (e) Saundeers, W. H., Jr.; Van Verth, J. E. Ab initio comparison of identity-reaction proton transfers from carbon acids yielding localized vs delocalized caonjugate bases. *J. Org. Chem.* **1995**, *60*, 3452–3458. (f) Benham, S. M.; Benham, S. E.; Ando, K.; Green, N. S.; Houk, K. N. Stereoelectronic, torsional, and steric effects on rates of enolization of ketones. *J. Org. Chem.* **2000**, 8970–8978.
- 58 Stanton, J. F.; Gauss, J.; Watts, J. D.; Lauderdale, W. J.; Bartlett, R. J. The ACES II program system. *Int. J. Quantum Chem., Quantum Chem. Symp.* **1992**, *26*, 879–894.
- 59 Lynch, T. J.; Newcomb, M.; Bergbreiter, D. E.; Hall, M. B. Molecular structure of the lithium enolate of acetaldehyde. *J. Org. Chem.* **1980**, *45*, 5005–5006.
- 60 Ren, J.; Cramer, C. J.; Squires, R. R. Superacidify and superelectrophilicity of  $BF_3$ -carbonyl complexes. *J. Am. Chem. Soc.* **1999**, *121*, 2633–2634.
- 61 Snowden, T. S.; Anslyn, E. V. Artificial receptors for enolizations and  $pK_a$  shifts. *Bioorg. Med. Chem.* **2001**, *9*, 2467–2478.
- 62 Sandro, G.; Colin, T. Acyl-CoA dehydrogenases: A mechanistic overview. *Eur. J. Biochem.* **2004**, *271*, 494–508.
- 63 Kim, J. J. P.; Retsu, M. Acyl-CoA dehydrogenases and acyl-CoA oxidases. Structural basis for mechanistic similarities and differences. *Eur. J. Biochem.* **2004**, *271*, 484–493.